# Quantum propagation of neutral atoms in a magnetic quadrupole guide

Article (Published Version)

# Quantum propagation of neutral atoms in a magnetic quadrupole guide

E. A. Hinds and Claudia Eberlein
*Sussex Centre for Optical and Atomic Physics, University of Sussex, Falmer, Brighton BN1 9QH, England*
(Received 28 September 1999; published 17 February 2000)

We consider the quantized motion of neutral atoms at very low temperature in a two-dimensional magnetic quadrupole structure formed, for example, by four current-carrying wires along the $z$ direction. The magnetic field **B** in the guide is proportional to the vector $(x,-y)$. We show that this field can be used to make a single-mode atomic de Broglie waveguide which has bound states of low angular momentum, even though the field at the center of the guide goes to zero. We investigate the spectrum and decay rate of the transverse modes for spin-1/2 and spin-1 atoms.

PACS number(s): 03.75.Be, 03.65.−w, 42.50.−p

## I. INTRODUCTION AND MOTIVATION

For the last decade it has been possible to cool atoms from room temperature (atom velocity 500 m/s) to $\mu$K temperatures (velocity 1 cm/s) by using light beams to provide the very strong friction required [1]. Optical forces can also be used to confine or guide cold atoms [2, 3]. For example, long cylindrical atom guides have been made from hollow optical fibers, with the light propagating in the glass tuned far to the blue of the atomic resonance. The evanescent light field within the hollow center decays exponentially away from the wall, producing a repulsive optical dipole force [4] which guides atoms along the center [5]. Alternatively, red-detuned light propagating in the hollow center of the fiber can also be used to guide atoms [6]. One disadvantage of optical confinement is the heating caused by laser fluctuations and by spontaneous emission. This can be avoided by using static fields to confine or guide the atoms [7]. Magnetostatic traps [8] provided the stable environment required for evaporative cooling [9] of atomic vapors, which led eventually to Bose-Einstein condensation [10]. In the same way, magnetostatic fields seem to offer the best prospect for making single-mode cylindrical waveguides for atomic de Broglie waves.

The earliest magnetic atom guide was demonstrated by Friedburg and Paul [11], who used six current bars carrying several hundred A each to approximate a magnetic hexapole. There the magnitude of the field grows quadratically with distance from the axis, which binds weak-field-seeking atoms in an approximately harmonic potential and allows a thermal atomic beam to be focused. With the advent of cold atoms, several other magnetic guides were proposed. One idea was to bind strong-field-seeking atoms to Kepler orbits around a current-carrying wire [12]. This was demonstrated in the laboratory [13], but does not easily lend itself to the guiding of atomic de Broglie waves in a single low-order mode because the atom must be kept away from the wire by having a high angular momentum. In another recently proposed guide [14], two helical solenoids are interleaved on the same radius and carry equal but opposite currents. This arrangement generates a low field in the center which rises rapidly near the walls at a rate determined by the pitch of the windings. The guiding potential is very similar to that of the hollow optical fiber, but again, single-mode guiding seems unlikely as it would be difficult to build this structure with small enough radius to separate the low-order transverse eigenmodes. The most promising idea for single-mode guiding seems to be the magnetic quadrupole guide in which the magnitude of the magnetic field is zero on the cylindrical symmetry axis and increases linearly with distance from the axis [7].

A quadrupole guide can be elegantly achieved by using a single current-carrying wire together with a uniform bias field perpendicular to the wire. The uniform field and the field produced by the wire cancel each other along a line parallel to the wire, which becomes the axis of the guide. In a Taylor expansion around this zero, the field strength increases linearly which results in a quadrupole guide potential. Classical guiding of atoms in such a potential has been demonstrated [15], but no experiment has yet approached the limit of single-mode propagation in any multipole structure. In our laboratory in Sussex we have built a quadrupole guide with four straight wires which are parallel to the $z$ axis and intersect the $x$-$y$ plane at the corners of a square at $(\pm R/\sqrt{2}, \pm R/\sqrt{2})$. They carry currents $+I$ and $-I$ alternately so that those on the same diagonal have the current flowing in the same direction. From Ampère's law it is easy to work out the magnetic field created by this configuration. A Taylor expansion around the center $(x=0, y=0)$ then yields

$$B_x \approx 4B_0 \frac{x}{R}, \quad B_y \approx -4B_0 \frac{y}{R}, \tag{1.1}$$

where $B_0 = \mu_0 I/(2\pi R)$. This gives a field strength which increases linearly with distance $\rho = (x^2+y^2)^{1/2}$ from the axis of the guide. If we increase the number of wires to six, we obtain the Friedburg/Paul hexapole with a field near the center of

$$B_x \approx 6B_0\left(\frac{x^2}{R^2} - \frac{y^2}{R^2}\right), \quad B_y \approx -12B_0 \frac{xy}{R^2},$$

and the strength of the field increases quadratically with $\rho$. Higher multipoles produce even weaker field variation near the center and are therefore less useful for achieving large separation of the transverse de Broglie wave modes.

 

Atoms constrained to propagate in a single-mode waveguide are interesting from the point of view of atom optics and interferometry because the phase of the de Broglie wave can in principle be preserved over macroscopic propagation lengths. A quantum gas confined to a line is also interesting as a physical system in its own right. It has been proposed that such a system would be a realization of a so-called ''Tonks'' gas whose elementary excitations obey Fermi statistics even though it consists of bosons [16]. There has also been a suggestion that a trapped one-dimensional Bose gas would exhibit Luttinger liquid behavior and have correlation functions that decay algebraically [17].

In the rest of this paper, we consider the quantum mechanics of a single atom propagating in a quadrupole guide. Our main interests are to establish the spectrum of the lowest few states, to determine if any of them are stable, and to understand the connection between the adiabatic approximation and the real evolution. We begin by formulating the Schrödinger equation for this problem, then in Sec. III we analyze the special case of a spin-1/2 atom. Section IV concerns the more general problem of spin 1. In Secs. V and VI we discuss why atoms are lost at the center of the guide as a result of spin-flip transitions and we comment on the stabilization of the guide by means of an additional field along the axis. Our concluding remarks are presented in Sec. VII. The Appendix explains how one determines phase shifts and lifetimes of quasibound states in a quadrupolar potential.

## II. SCHRÖDINGER EQUATION

The linear Zeeman interaction between the atom and the magnetic field takes the form

$$V = g\mu_B \mathbf{s}\cdot\mathbf{B},$$

where $\mathbf{s}$ is the total angular momentum of the atom, $g$ is the Landé $g$ factor and $\mu_B$ is the Bohr magneton. For the field strengths of interest to us, this linear approximation is valid because the interaction is small compared with any fine or hyperfine splittings. In this case, the nonrelativistic motion of the atom in the guide is described by the Schrödinger equation for the $(2s+1)$ component spinor wave function $\psi$ [18]

$$i\frac{\partial\psi(\vec{r},t)}{\partial t} = \left(\frac{\mathbf{p}^2}{2m} + V\right)\psi(\mathbf{r},t).$$

Since $V$ depends only on $x$ and $y$, the problem is translation invariant along the $z$ axis. The wave function is simply the product of a plane wave with momentum $p_z$ in $z$ direction and an $(x,y)$-dependent part:

$$\psi(\mathbf{r},t) = e^{i[p_z z - (p_z^2/2m)t]}\psi(x,y,t).$$

The motion of the atom is therefore essentially described by the two-dimensional Schrödinger equation in the $x$-$y$ plane

$$i\frac{\partial\psi(x,y,t)}{\partial t} = \left[-\frac{1}{2m}(\nabla_x^2+\nabla_y^2) + V(x,y)\right]\psi(x,y,t), \tag{2.1}$$

which we will consider from now on.

Before attempting to find eigenmodes of Eq. (2.1), we would like to make some general remarks about the potential in this equation. A spin in a constant magnetic field precesses around the field with the Larmor frequency, maintaining a constant spin component $m_s$ along the field. If the field changes in direction or magnitude, $m_s$ remains adiabatically invariant provided the rate of change is small compared with the Larmor precession frequency. In that case, once $m_s$ is fixed, the Zeeman energy $g\mu_B m_s|B|$ depends only on the magnitude of the magnetic field, $|B(x,y)|$. Thus one might expect an atom with positive $gm_s$ to move in a quadrupole field as if it were a spinless particle in a linear binding potential $G\rho$, where $G = 4g\mu_B m_s B_0/R$ is the energy gradient characterizing the adiabatic quadrupole potential. Similarly, in a hexapole field one might expect the motion to be described by a harmonic adiabatic potential proportional to $(\rho/R)^2$. It is the steepness of the linear potential that makes it attractive for achieving a large separation of the low-order modes in a de Broglie waveguide. However, this adiabatic picture is not reliable in regions where the field strength goes to zero because the Larmor precession frequency vanishes there, allowing $m_s$ to change. For example, it is well known [19] that atoms held in a spherical quadrupole trap escape as a result of spin flips occurring near the center, where the magnetic field vanishes. A similar problem is to be expected in magnetic quadrupole guides and in guides of higher multipolarity. Nevertheless, there could still be stable guide modes in which the probability of finding the atom near the axis goes to zero. This paper was motivated by the wish to understand the leaking more clearly and to determine whether there are in fact any stable bound states in a quadrupole waveguide. As we shall show below, there are.

## III. SPIN 1/2

For spin $s=1/2$ the wave function $\psi(x,y,t)$ is a two-component spinor and the spin matrices are $\mathbf{s}=\boldsymbol{\sigma}/2$ with $\boldsymbol{\sigma} = (\sigma_x,\sigma_y,\sigma_z)$ being the Pauli matrices. Hence the potential is given by

$$V = G\begin{pmatrix} 0 & x+iy \\ x-iy & 0 \end{pmatrix} = G\rho\begin{pmatrix} 0 & e^{i\phi} \\ e^{-i\phi} & 0 \end{pmatrix}. \tag{3.1}$$

We are now interested in finding eigensolutions of the stationary Schrödinger equation which reads in polar coordinates

$$2mE\psi(\rho,\phi) = \left(-\frac{\partial^2}{\partial\rho^2} - \frac{1}{\rho}\frac{\partial}{\partial\rho} - \frac{1}{\rho^2}\frac{\partial^2}{\partial\phi^2} + 2mV\right)\psi(\rho,\phi), \tag{3.2}$$

where the energy $E$ is an eigenvalue of the transverse motion.

Let us imagine a state where the atom is everywhere spin-up relative to the local direction of the magnetic quadrupole field. This is obviously a bound state in the adiabatic approximation. In order to construct such a state we first note that when the atom is on the positive $x$ axis, the local field is

along $+x$ and therefore this state has its spin along $+x$. More generally, at position $(\rho,\phi)$, the angle between the field vector and the $x$ axis is $-\phi$, as can be found from Eq. (1.1), and therefore the spin in this state also makes an angle $-\phi$ to the $x$ axis. Hence the local spin-up state we want can be generated by starting with a spin $\binom{1}{0}$ that points along $+z$, rotating it by $\pi/2$ around the $y$ axis to transform it into a spin along $+x$, and subsequently rotating it by $-\phi$ around the $z$ axis. These rotations can be performed by the standard rotation matrix [20], [Sec. 2.4]

$$\mathcal{D}^{1/2}_{mm'}\left(0,\frac{\pi}{2},-\phi\right)=\left\langle m\left|\exp\left(-i\frac{\pi}{2}s_y\right)\exp(i\phi s_z)\right|m'\right\rangle = \begin{pmatrix} \frac{1}{\sqrt{2}}e^{i\phi/2} & -\frac{1}{\sqrt{2}}e^{i\phi/2} \\ \frac{1}{\sqrt{2}}e^{-i\phi/2} & \frac{1}{\sqrt{2}}e^{-i\phi/2} \end{pmatrix}. \tag{3.3}$$

Hence the spinor that describes the local spin-up state is

$$|\uparrow\rangle=\mathcal{D}^{1/2}_{mm'}\left(0,\frac{\pi}{2},-\phi\right)\begin{pmatrix}1\\0\end{pmatrix}=\frac{1}{\sqrt{2}}\begin{pmatrix}e^{i\phi/2}\\e^{-i\phi/2}\end{pmatrix}. \tag{3.4}$$

Similarly, the spin-down state is

$$|\downarrow\rangle=\frac{1}{\sqrt{2}}\begin{pmatrix}-e^{i\phi/2}\\e^{-i\phi/2}\end{pmatrix}.$$

In general, the wave function must be a superposition of spin-up and spin-down states. If there is no orbital angular momentum this can be written as

$$\psi(\rho,\phi)=\frac{1}{\sqrt{2}}\begin{pmatrix}f_+(\rho)e^{i\phi/2}\\f_-(\rho)e^{-i\phi/2}\end{pmatrix}, \tag{3.5}$$

where $f_+$ and $f_-$ are equal in a pure spin-up state, and equal and opposite in a pure spin-down state. Inserting this into Eq. (3.2) one obtains the two equations

$$\left(-f_+''-\frac{f_+'}{\rho}+\frac{f_+}{4\rho^2}\right)e^{i\phi/2}+2mG\rho f_-e^{i\phi/2}=2mEf_+e^{i\phi/2},$$

$$\left(-f_-''-\frac{f_-'}{\rho}+\frac{f_-}{4\rho^2}\right)e^{-i\phi/2}+2mG\rho f_+e^{-i\phi/2}=2mEf_-e^{-i\phi/2}, \tag{3.6}$$

from which the $\phi$ dependence evidently cancels out. This is a great simplification of the problem. Whereas the components of Eq. (3.2) were coupled partial differential equations requiring sophisticated methods for their solution, these are ordinary (though still coupled) differential equations, which can always be solved by a simple Runge-Kutta routine.

If we allow the atom to have orbital angular momentum around the center of the guide, i.e., the $z$ axis, Eq. (3.5) becomes

$$\psi(\rho,\phi)=\frac{1}{\sqrt{2}}\begin{pmatrix}F_+(\rho)e^{i(\ell+1/2)\phi}\\F_-(\rho)e^{i(\ell-1/2)\phi}\end{pmatrix},$$

where $\ell$ is an integer. Then the $\phi$ dependence of Eq. (3.2) still decouples, and for the radial functions we obtain the two ordinary differential equations:

$$-F_+''-\frac{F_+'}{\rho}+\frac{\left(\ell+\frac{1}{2}\right)^2F_+}{\rho^2}+2mG\rho F_-=2mEF_+,$$

$$-F_-''-\frac{F_-'}{\rho}+\frac{\left(\ell-\frac{1}{2}\right)^2F_-}{\rho^2}+2mG\rho F_+=2mEF_-. \tag{3.7}$$

### A. Solutions for $\ell=0$

For $\ell=0$ the system of differential equations to be solved is Eq. (3.6). These decouple if, instead of $f_+(\rho)$ and $f_-(\rho)$, one considers the radial function $v(\rho)=f_+(\rho)+f_-(\rho)$, which corresponds to spin-up, and the function $w(\rho)=f_+(\rho)-f_-(\rho)$, which describes the spin-down component,

$$-v''-\frac{v'}{\rho}+\frac{v}{4\rho^2}+2mG\rho v=2mEv,$$

$$-w''-\frac{w'}{\rho}+\frac{w}{4\rho^2}-2mG\rho w=2mEw. \tag{3.8}$$

Substituting $v=\tilde{v}/\sqrt{\rho}$ and $w=\tilde{w}/\sqrt{\rho}$, one finds

$$-\tilde{v}''+2mG\rho\tilde{v}=2mE\tilde{v},$$

$$-\tilde{w}''-2mG\rho\tilde{w}=2mE\tilde{w}.$$

These are Airy equations whose general solutions are [21, Sec. 10.4]

$$\tilde{v}(\rho)=c_1\,\mathrm{Ai}\left[(2mG)^{1/3}\left(\rho-\frac{E}{G}\right)\right]+c_2\,\mathrm{Bi}\left[(2mG)^{1/3}\left(\rho-\frac{E}{G}\right)\right],$$

$$\tilde{w}(\rho)=d_1\,\mathrm{Ai}\left[-(2mG)^{1/3}\left(\rho+\frac{E}{G}\right)\right]+d_2\,\mathrm{Bi}\left[-(2mG)^{1/3}\left(\rho+\frac{E}{G}\right)\right].$$

Since $\mathrm{Bi}(\zeta)$ grows exponentially for large $\zeta$, the coefficient $c_2$ must be set to zero, as the wave function is otherwise not normalizable. In addition, physical quantities must be regular

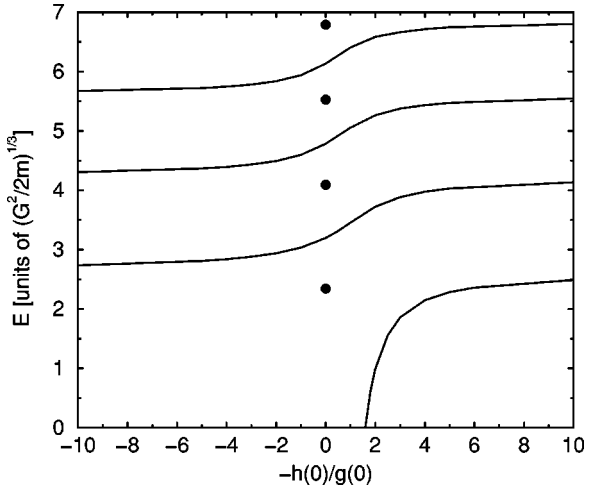


FIG. 1. Lines: lowest four bands of $s=1/2, \ell=1$ spectrum versus boundary condition at the origin. Dots: first four $s=1/2, \ell=0$ bound state energies. For these states $\lim_{\xi\to 0} h(\xi)/g(\xi) \propto \xi \to 0$.

at $\rho=0$. Since $f_\pm=(\tilde{v}\pm\tilde{w})/(2\sqrt{\rho})$, the probability density $\psi^\dagger\psi$ is always integrable with respect to $\int d\rho\rho\int d\phi$, but the momentum density

$$-i\psi^\dagger\nabla\psi=-i\psi^\dagger\left(\hat{\mathbf{e}}_\rho\frac{\partial}{\partial\rho}+\hat{\mathbf{e}}_\phi\frac{1}{\rho}\frac{\partial}{\partial\phi}\right)\psi \tag{3.9}$$

is not, unless one requires $\tilde{v}(0)=0$ and $\tilde{w}(0)=0$. This restricts the eigenvalues $E$ to discrete values given by the zeros of the Airy functions. The discreteness of $E$ then enforces $d_1=0$ and $d_2=0$, and consequently $\tilde{w}=0$, because the asymptotic behavior of the Airy functions of negative arguments is oscillatory $[\mathrm{Ai}(-z)\sim\pi^{-1/2}z^{-1/4}\sin(2z^{3/2}/3+\pi/4)$ and $\mathrm{Bi}(-z)\sim\pi^{-1/2}z^{-1/4}\cos(2z^{3/2}/3+\pi/4)]$. This would be admissible for traveling eigenstates with continuous eigenvalues but not for eigenfunctions that belong to discrete eigenvalues.

In summary, for $\ell=0$ there exist bound states and they correspond to local spin-up states. (We have taken the $g$ factor $g$, and therefore the characteristic energy gradient $G$, to be positive. With negative $g$ the bound states are spin-down.) The bound-state energies $E_n$ are given by the zeros of the Airy function Ai [22]

$$\mathrm{Ai}\left[-\left(\frac{2mG}{\hbar^2}\right)^{1/3}\frac{E_n}{G}\right]=0.$$

These zeros are tabulated in [21, Table 10.13]; the first few are

$$\left(\frac{2mG}{\hbar^2}\right)^{1/3}\frac{E_n}{G}=2.338, 4.088, 5.521, 6.787, \ldots . \tag{3.10}$$

The corresponding eigenfunctions $|\psi_i\rangle$ are $|\uparrow\rangle$ spinors of the form (3.5):

$$|\psi_n\rangle=\mathcal{N}\frac{1}{\sqrt{\rho}}\mathrm{Ai}\left[\left(\frac{2mG}{\hbar^2}\right)^{1/3}\left(\rho-\frac{E_n}{G}\right)\right]|\uparrow\rangle,$$

where $\mathcal{N}$ is a normalization constant.

### B. Solutions for $\ell>0$

For $\ell>0$ one has to solve the system (3.7) which no longer decouples into spin-up and spin-down parts because the two terms involving $1/\rho^2$ are now different. However, the equations can readily be integrated by using a standard Runge-Kutta numerical routine.

To this end, we need to establish the boundary conditions for $F_\pm(\rho)$ near $\rho=0$. For small $\rho$ one can neglect the potential terms proportional to $\rho$ on the left-hand sides and the energy terms on the right-hand sides of Eq. (3.7). A power series expansion for $F_\pm(\rho)$ around $\rho=0$ then yields the limiting behavior $F_\pm(\rho)\propto\rho^{\ell\pm1/2}$ near the origin. Hence we substitute into Eq. (3.7) $F_+(\rho)=\rho^{\ell+1/2}g(\rho)$ and $F_-(\rho)=(2mG)^{-1/3}\rho^{\ell-1/2}h(\rho)$, and at the same time we change to the dimensionless variable $\xi=(2mG)^{1/3}\rho$, to obtain

$$-g''-2(\ell+1)\frac{g'}{\xi}+h=(2mG)^{1/3}\frac{E}{G}g$$

$$-h''-2\ell\frac{h'}{\xi}+\xi^2 g=(2mG)^{1/3}\frac{E}{G}h. \tag{3.11}$$

Near the origin both $g$ and $h$ must behave as [const $+O(\xi^2)$]: they cannot have terms linear in $\xi$ because $g'/\xi$ and $h'/\xi$ would become irregular for $\xi\to0$. Hence one can integrate Eq. (3.11) numerically, taking $g(0)$, $h(0)$ as constants and setting $g'(0)$, $h'(0)$ to zero as the initial conditions. Since the normalization of the wave function is a further restriction on $g$ and $h$, the only free parameter that remains is the ratio $h(0)/g(0)$. By varying this ratio between $-\infty$ and $+\infty$ one can sweep the complete space of possible solutions.

The energy eigenvalues $E$ are determined by the shooting method. This involves choosing some number for $E$ and integrating Eq. (3.11). If the chosen number is not an eigenvalue the solution diverges at large $\xi$. When $E$ is varied and crosses an eigenvalue, the sign of the divergence changes because the number of nodes of the wave function changes by 1 at each successive eigenvalue. Hence repeated bisections converge on the eigenvalues to any desired accuracy. The spectrum determined in this way consists of continuous bands of eigenvalues. For $\ell=1$ the lowest few bands are plotted in Fig. 1 as a function of $-h(0)/g(0)$. This ratio is infinite when $g(0)=0$, but then all nonzero initial values specified for $h(0)$ are equivalent because the resulting wave functions differ at most by a phase factor. In other words, the points $+\infty$ and $-\infty$ on the $-h(0)/g(0)$ axis are equivalent so that the bands are really one continuous but multivalued function of the initial conditions. For higher $\ell$ these bands are shifted to higher energies. For example, the first complete $\ell=1$ band in Fig. 1 ranges from 2.629 946 to 4.224 64

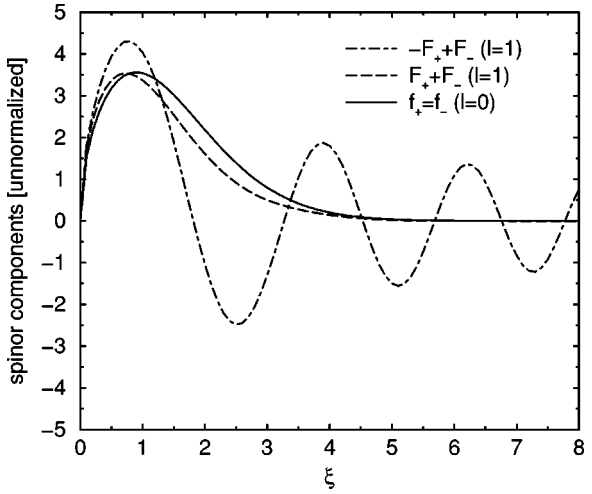


FIG. 2. Solid line: wave function for $s=1/2, \ell=0$ ground state. Also shown are the spin-up (dashed line) and spin-down (dot-dashed line) components of the wave function for the $s=1/2, \ell=1$ state of the same energy.

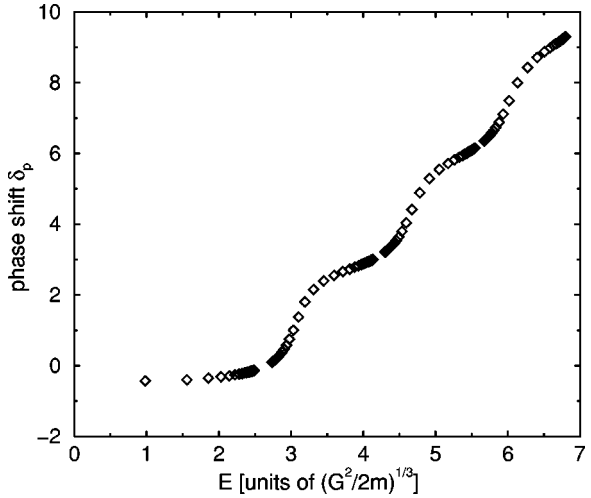


FIG. 3. Plot of the phase shift $\delta_p$ as a function of energy $E$ for $s=1/2$, $\ell=1$. The steps in $\delta_p$ are not particularly sharp, which means that the resonances are fairly wide and indicates that the lifetime of the quasibound states is comparable with the oscillation period in the guide.

$(G^2/2m)^{1/3}$, whereas the equivalent band for $\ell=2$ is shifted to $3.779\,654\,7\ldots5.153\,145\,(G^2/2m)^{1/3}$.

The $\ell=1$ states are very different from those for $\ell=0$. In the region near the origin, where $\rho \ll (2mG)^{-1/3}|h(0)/g(0)|$, the wave function becomes proportional to $\sqrt{\rho}e^{i\phi/2}\binom{0}{1}$, and the spin points along the $-z$ direction, that is, along the axis of the guide and antiparallel to $\ell$. It is therefore a superposition of equal $|\uparrow\rangle$ and $|\downarrow\rangle$ amplitudes. Further out, the spin-up part, being bound, decreases exponentially, while the spin-down component oscillates to infinity. This is illustrated in Fig. 2, which shows the $\ell=0$ ground-state wave function (solid line) together with the $|\uparrow\rangle$ (dashed line) and $|\downarrow\rangle$ (dot-dashed line) components of the wave function for the $\ell=1$ state of the same energy, namely, $2.338\ (G^2/2m)^{1/3}$.

Each band in Fig. 1 exhibits a steep rise near the center of the figure, i.e., around $h(0)/g(0)\approx 0$, which is where the resonances of the guide occur. The first step, which begins at zero energy, corresponds to the turning on of the first transverse mode and the appearance of a single peak in the spin-up part of the wave function as shown in Fig. 2. The next step, near $E\approx 3$, corresponds to the appearance of the first node in the spin-up wave function, and each subsequent step heralds the appearance of another lobe in the transverse bound state. Roughly in the middle of each step there occurs a resonance, which is to say that at these energies there exist quasibound states of a limited lifetime. These resonances can be seen as phase shifts in the spin-down component of the wave function. However, while the calculation of phase shifts is a standard technique for analyzing resonances, its application to the system at hand is not straightforward because the potential generated by the field (1.1) rises linearly towards infinity so that even far away from the center, where the spin components decouple from each other, they do not form plane waves. The Appendix explains how wave packets can be constructed in such a nonlinear system and how one can calculate phase shifts by following the change of position of zeros in the spin-down wave function with energy. For $s=1/2, \ell=1$ the dependence of the phase shift on energy is plotted in Fig. 3. Fitting the data of Fig. 3 to a sum of arctan steps of the form (A10), we have determined the energies and widths $(\epsilon_i, \Gamma_i)$ of the first three resonances for $\ell=1$ as (3.07,0.19), (4.66,0.23), and (6.12,0.3). Doing the same for $\ell=2$ one obtains the values (3.94,0.07), (5.36,0.1), and (6.8,0.15). In either case, the widths indicate that these quasibound $s=1/2$ states are rapidly decaying, with a lifetime comparable to the oscillation period of the atoms in the guide.

## IV. SPIN 1

The behavior of a spin $s=1$ is qualitatively different from that of a spin 1/2 because a $s=1$ spinor has three components instead of two. The atom-field interaction potential is

$$V=\sqrt{2}G\rho\begin{pmatrix} 0 & e^{i\phi} & 0 \\ e^{-i\phi} & 0 & e^{i\phi} \\ 0 & e^{-i\phi} & 0 \end{pmatrix}. \tag{4.1}$$

Following the same ideas as for spin 1/2 we take the $m_z=+1$ eigenspinor, rotate it by $\pi/2$ around the $y$ axis so that it lies along $+x$, then rotate it by $-\phi$ around the $z$ axis. For $s=1$ the rotation matrix is [20, Sec. 2.4]

$$\mathcal{D}^1_{mm'}\left(0,\frac{\pi}{2},-\phi\right)=\frac{1}{2}\begin{pmatrix} e^{i\phi} & -\sqrt{2}e^{i\phi} & e^{i\phi} \\ \sqrt{2} & 0 & -\sqrt{2} \\ e^{-i\phi} & \sqrt{2}e^{-i\phi} & e^{-i\phi} \end{pmatrix}. \tag{4.2}$$

This gives the spin-up state for spin 1 at position $(\rho,\phi)$ as

$$|\uparrow\rangle = \mathcal{D}^1_{mm'}\left(0, \frac{\pi}{2}, -\phi\right)\begin{pmatrix}1\\0\\0\end{pmatrix} = \frac{1}{2}\begin{pmatrix}e^{i\phi}\\\sqrt{2}\\e^{-i\phi}\end{pmatrix}. \quad (4.3)$$

Similarly, the spin-down state is

$$|\downarrow\rangle = \frac{1}{2}\begin{pmatrix}e^{i\phi}\\-\sqrt{2}\\e^{-i\phi}\end{pmatrix},$$

and the state that everywhere has $m=0$ relative to the local field is

$$|0\rangle = \frac{1}{\sqrt{2}}\begin{pmatrix}-e^{i\phi}\\0\\e^{-i\phi}\end{pmatrix}. \quad (4.4)$$

As before, we now look for angular momentum eigenstates of Eq. (3.2) [but now with the potential (4.1)] that are $\rho$-dependent superpositions of the three adiabatic spin states:

$$\psi(\rho,\phi) = \frac{1}{2}e^{i\ell\phi}\begin{pmatrix}f_+(\rho)e^{i\phi}\\\sqrt{2}f_0(\rho)\\f_-(\rho)e^{-i\phi}\end{pmatrix}. \quad (4.5)$$

In the following we shall concentrate on the case $\ell=0$ and refrain from a detailed discussion of $\ell>0$ as for spin 1 there are no qualitative differences between the two cases. Using Eq. (4.5) with $\ell=0$, we find that the stationary Schrödinger equation is turned into the system

$$-f_+'' - \frac{f_+'}{\rho} + \frac{f_+}{\rho^2} + 4mG\rho f_0 = 2mEf_+, \quad (4.6a)$$

$$-f_0'' - \frac{f_0'}{\rho} + 4mG\frac{\rho}{2}(f_+ + f_-) = 2mEf_0, \quad (4.6b)$$

$$-f_-'' - \frac{f_-'}{\rho} + \frac{f_-}{\rho^2} + 4mG\rho f_0 = 2mEf_-. \quad (4.6c)$$

Since the first and the last of these equations are of the same form, we rewrite this system by considering the sum and the difference of Eqs. (4.6a) and (4.6c). In terms of $f_1=(f_+ + f_-)/2$ and $f_2=f_+ - f_-$ we get

$$-f_1'' - \frac{f_1'}{\rho} + \frac{f_1}{\rho^2} + 4mG\rho f_0 = 2mEf_1, \quad (4.7a)$$

$$-f_0'' - \frac{f_0'}{\rho} + 4mG\rho f_1 = 2mEf_0, \quad (4.7b)$$

$$-f_2'' - \frac{f_2'}{\rho} + \frac{f_2}{\rho^2} = 2mEf_2. \quad (4.7c)$$

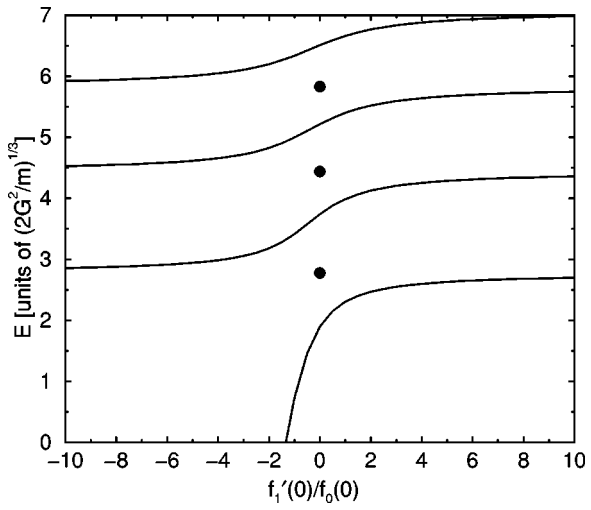


FIG. 4. Solid lines: lowest four bands of the $s=1,\ell=0$ spectrum. Dots: the first three $s=1,\ell=0$ bound states. For these states $f_1'(0)/f_0(0)\to 0$.

The function $f_2$ is the radial wave function for the spin component $|0\rangle$ of Eq. (4.4), which is why there is no potential energy term in Eq. (4.7c). Since this component is unbound, it must vanish in the bound states we are seeking.

We now turn to the remaining two equations, Eqs. (4.7a) and (4.7b). Since they do not readily separate, we shall integrate them numerically. In preparation for this we adopt the new natural length scale $(4mG/\hbar^2)^{-1/3}$ and make the substitution $\zeta=(4mG/\hbar^2)^{1/3}\rho$ to obtain the system of equations

$$-f_1''(\zeta) - \frac{f_1'(\zeta)}{\zeta} + \frac{f_1(\zeta)}{\zeta^2} + \zeta f_0(\zeta) = \frac{1}{2}(4mG)^{1/3}\frac{E}{G}f_1(\zeta)$$

$$-f_0''(\zeta) - \frac{f_0'(\zeta)}{\zeta} + \zeta f_1(\zeta) = \frac{1}{2}(4mG)^{1/3}\frac{E}{G}f_0(\zeta). \quad (4.8)$$

Once again the behavior near $\zeta=0$ can be found by a power-series expansion:

$$f_0(\zeta) \overset{\zeta\to 0}{\sim} \text{const} + O(\zeta^2) \quad \text{and} \quad f_1(\zeta) \overset{\zeta\to 0}{\sim} \text{const}'\,\zeta + O(\zeta^3). \quad (4.9)$$

Consequently, our initial conditions for the Runge-Kutta integration are constant $f_0(0)$, zero $f_0'(0)$, zero $f_1(0)$, and constant $f_1'(0)$. Again, the normalization of the wave function takes away one free parameter, so that the energy eigenvalue is completely determined by the ratio $f_1'(0)/f_0(0)$. When we sweep this from $-\infty$ to $\infty$, the numerical integration again yields bands which cover the whole range of real positive energies $E$. The four lowest bands are plotted in Fig 4. Once again there is a step in each band which coincides with the appearance of a new transverse lobe in the spin-up part of the wave function. All these states have a non-negligible spin-down component at large $\rho$, which corresponds to the loss of the atom from the waveguide within a few oscillation periods.

It may seem that this exhausts the spectrum of physical eigenstates but the power-series expansion that has led to the initial conditions (4.9) does not in fact cover all possible cases. As $\zeta \to 0$ the potential terms proportional to $\zeta$ can be neglected, so that Eq. (4.8) separates into two equations of the form

$$-f_\nu''(\zeta) - \frac{f_\nu'(\zeta)}{\zeta} + \nu^2 \frac{f_\nu(\zeta)}{\zeta^2} = \epsilon f_\nu(\zeta), \tag{4.10}$$

with $\nu = 0,1$ and $\epsilon = (2G^2/m)^{-1/3}E$. These are Bessel's equations. Hence for small $\zeta$ one finds the general solutions

$$f_0(\zeta) \sim \{J_0(\sqrt{\epsilon}\zeta), Y_0(\sqrt{\epsilon}\zeta)\} \tag{4.11a}$$

$$f_1(\zeta) \sim \{J_1(\sqrt{\epsilon}\zeta), Y_1(\sqrt{\epsilon}\zeta)\}. \tag{4.11b}$$

The $J_0$ and $J_1$ solutions coincide with the initial conditions (4.9). The $Y_1$ solution can be ruled out because it behaves as $1/\zeta$ for small $\zeta$ and hence is irregular. However, $Y_0$ close to the origin has the form [21, Sec. 9.1.13]

$$\lim_{z \to 0} Y_0(z) = \frac{2}{\pi}\left[\ln\left(\frac{z}{2}\right) + \gamma\right] + O(z^2 \ln z, z^2), \tag{4.12}$$

where $\gamma \approx 0.5772$ is Euler's constant. This means that $Y_0$ in Eq. (4.11a) is a physically acceptable solution: $\ln \rho$ is integrable under $\int d\rho \rho \int d\phi$ and the momentum density (3.9) is likewise integrable for such solutions.

To see if there are any bound states that behave as $Y_0$ at the origin, we integrate numerically inward, starting at a large value of the argument $\zeta$. The asymptotic behavior at large $\zeta$ can be found by considering the sum $f_1 + f_0$ and difference $f_1 - f_0$, which are the radial functions for the spin-up and spin-down parts of the wave function. We see from Eq. (4.8) that they do not separate because of the term $f_1(\zeta)/\zeta^2$ in the first equation. However, as $\rho \to \infty$ this term can be neglected, and for $\rho \gg E/G$ we obtain

$$(f_1 + f_0)'' + \frac{(f_1 + f_0)'}{\zeta} - \zeta(f_1 + f_0) = 0,$$

$$(f_1 - f_0)'' + \frac{(f_1 - f_0)'}{\zeta} + \zeta(f_1 - f_0) = 0.$$

With the substitution $\eta = 2/3\zeta^{3/2}$ both of these become Bessel's equation with index 0. Therefore the general asymptotic solutions are [21, Secs. 9.1,9.6]

$$(f_1 + f_0) \sim \left\{ I_0\left(\frac{2}{3}\zeta^{3/2}\right), K_0\left(\frac{2}{3}\zeta^{3/2}\right)\right\} \tag{4.13a}$$

$$(f_1 - f_0) \sim \left\{ J_0\left(\frac{2}{3}\zeta^{3/2}\right), Y_0\left(\frac{2}{3}\zeta^{3/2}\right)\right\}. \tag{4.13b}$$

The spin-down $J_0$ and $Y_0$ solutions oscillate at large radius, as one would expect for unbound states. The spin-up solution proportional to $I_0$ grows exponentially for large arguments and must be ruled out as unphysical, but the $K_0$ solution falls exponentially at large $\rho$, as it should for a bound state. Thus for the state we are seeking, which is a bound spin-up state with an asymptotically negligible spin-down component, the boundary condition at large radius is

$$f_1(\zeta) \sim f_0(\zeta) \sim K_0\left(\frac{2}{3}\zeta^{3/2}\right) \sim \left(\frac{2}{3}\zeta^{3/2}\right)^{-1/2} \exp\left(-\frac{2}{3}\zeta^{3/2}\right).$$

This is used to specify the initial conditions for the Runge-Kutta integration at some point $\zeta \gg 0$. We then integrate Eq. (4.8) and vary the eigenvalue until $f_1(\zeta)$ converges towards the origin and $f_0(\zeta)$ diverges logarithmically, as prescribed by Eq. (4.12).

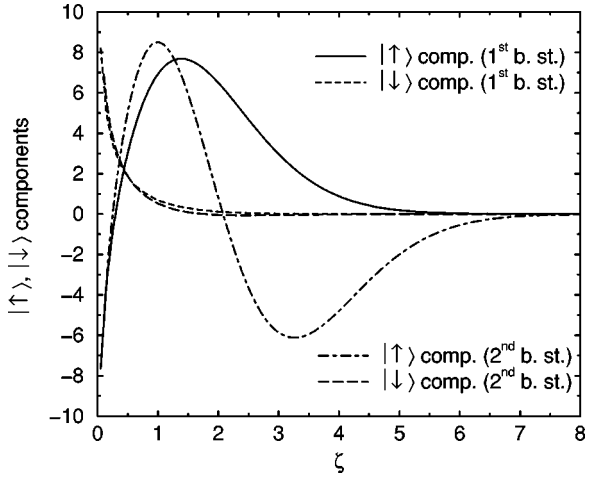


FIG. 5. Spinor components of the two lowest $s=1, \ell=0$ bound states.

We find that bound states of this kind do exist. The spinor wave functions of the first and the second are shown in Fig. 5. Since $f_1$ approaches zero near the origin (and since bound states also require $f_2 = 0$), the spin state near the center of the guide approaches pure $m_s = 0$ with respect to the $z$ axis, i.e., $(|\uparrow\rangle - |\downarrow\rangle)/\sqrt{2}$. Hence it lies in the $xy$ plane of the guide but has equal probability of being perpendicular or parallel to the local magnetic field. At larger radii, $f_1 \approx f_0$ and the spin state approaches $|\uparrow\rangle$, i.e., the spin lies in the $xy$ plane of the guide and is parallel to the local magnetic field. This is rather different from the case of spin 1/2 where the spin of the bound $\ell = 0$ states remains aligned along the local field all the way in to the center of the guide.

The energies of the first few bound states are

$$\left(\frac{m}{2\hbar^2 G^2}\right)^{1/3} E = 2.771, 4.4367, 5.827\,84, \ldots . \tag{4.14}$$

These are shown are shown as dots in Fig. 4. Their energies lie precisely at the junction of one continuous band with the next, i.e., at the band edges where the parameter $f_1'(0)/f_0(0)$ in Fig. 4 equals $\pm\infty$. At these points the continuum states

have $f_0(0)=0$, which makes them orthogonal in spin to the bound ones for which $f_0(\zeta)$ diverges logarithmically as $\zeta \to 0$.

## V. REASONS FOR THE BREAKDOWN OF THE ADIABATIC APPROXIMATION

As we have seen in the preceding two sections, the adiabatic states $|\uparrow\rangle,|\downarrow\rangle$, etc., which have constant $m_s$ relative to the local magnetic field, are not generally eigenstates of the Hamiltonian. The exception is $s=1/2,\ell=0$, which has a set of $|\uparrow\rangle$ bound states. There are also bound states for $s=1,\ell=0$, but these are of mixed character near the origin and evolve into the spin-up adiabatic state only at larger radii. Generally, the adiabatic states are coupled to each other near the origin, which gives rise to spin-flips and therefore to a loss of atoms from the guide. In this section we examine how and why the adiabatic states are coupled to each other.

First we note that these states are related to the free-space spin states $|S,m_s\rangle$ by $\{|\uparrow\rangle,|\downarrow\rangle,\ldots\}=\mathcal{R}|S,m_s\rangle$, where the rotation matrix $\mathcal{R}$ is that of Eq. (3.3) for spin 1/2 or Eq. (4.2) for spin 1 [cf. Eqs. (3.4) and (4.3)]. The matrix elements of the Hamiltonian in Eq. (3.2) taken between the adiabatic states are therefore $\langle S,m_s'|\mathcal{R}^{-1}H\mathcal{R}|S,m_s\rangle$. Of course, an equivalent way to view the problem is in the transformed frame with axes such that the spin is projected on the local magnetic-field direction. Here the adiabatic states are just $|S,m_s\rangle$ and the Hamiltonian is given by

$$\tilde{H}=\mathcal{R}^{-1}H\mathcal{R} =\mathcal{R}^{-1}\frac{1}{2m}\left(-\frac{\partial^2}{\partial\rho^2}-\frac{1}{\rho}\frac{\partial}{\partial\rho}-\frac{1}{\rho^2}\frac{\partial^2}{\partial\phi^2}+2mV\right)\mathcal{R}.$$

The transformation $R$ was chosen in the first place to make $\mathcal{R}^{-1}V\mathcal{R}$ diagonal. For example, with spin 1/2,

$$\mathcal{R}^{-1}V\mathcal{R}=\begin{pmatrix} G\rho & 0 \\ 0 & -G\rho \end{pmatrix}. \tag{5.1}$$

The two terms with $\rho$ derivatives in $\mathcal{R}^{-1}\nabla^2\mathcal{R}$ are also diagonal because the rotation does not depend on the distance from the axis, i.e., $\mathcal{R}$ and $\partial/\partial\rho$ commute. However, the third term is not diagonal after transformation and this is the interaction which couples the adiabatic states to each other:

$$\mathcal{R}^{-1}\frac{1}{2m\rho^2}\frac{\partial^2}{\partial\phi^2}\mathcal{R} =\frac{1}{2m\rho^2}\left(\frac{\partial^2}{\partial\phi^2}+2\mathcal{R}^{-1}\frac{\partial\mathcal{R}}{\partial\phi}\frac{\partial}{\partial\phi}+\mathcal{R}^{-1}\frac{\partial^2\mathcal{R}}{\partial\phi^2}\right). \tag{5.2}$$

For spin 1/2, where $\mathcal{R}$ is given by Eq. (3.3), and when acting on states of definite angular momentum, i.e., $\exp(i\ell\phi)|\uparrow\rangle$, and $\exp(i\ell\phi)|\downarrow\rangle$, one finds

$$\mathcal{R}^{-1}\frac{1}{2m\rho^2}\frac{\partial^2}{\partial\phi^2}\mathcal{R}=\frac{1}{2m\rho^2}\begin{pmatrix} -\left(\ell^2+\frac{1}{4}\right) & \ell \\ \ell & -\left(\ell^2+\frac{1}{4}\right) \end{pmatrix}. \tag{5.3}$$

This matrix is in fact diagonal when $\ell=0$, which is the reason the $\ell=0$ spin-up state is stable for spin 1/2. We note that this term in the Hamiltonian is essentially an angular momentum barrier, but it persists as $(1/2)^2/(2m\rho^2)$ even when there is no orbital angular momentum. This is geometrical in origin and expresses the fact that in the adiabatic state the spin must rotate once for each excursion around the center of the guide. This geometrical barrier ensures that the wave function vanishes at the origin, as we see in Fig. 2, and as it must if the adiabatic state is to be stable. For $\ell=1$ the off-diagonal elements of Eq. (5.3) mix the spin-up and spin-down components in such a way that no stable states can be found.

For spin 1, $\mathcal{R}$ is given by Eq. (4.2), and we obtain for the matrix acting on states of definite angular momentum,

$$\mathcal{R}^{-1}\frac{1}{2m\rho^2}\frac{\partial^2}{\partial\phi^2}\mathcal{R} =\frac{1}{2m\rho^2}\begin{pmatrix} -\left(\ell^2+\frac{1}{2}\right) & \sqrt{2}\ell & -\frac{1}{2} \\ \sqrt{2}\ell & -(\ell^2+1) & \sqrt{2}\ell \\ -\frac{1}{2} & \sqrt{2}\ell & -\left(\ell^2+\frac{1}{2}\right) \end{pmatrix}.$$

Once again we see that the $\rho^{-2}$ potential barrier includes a geometrical part associated with the adiabatic spin rotation around the axis, but now there is also an off-diagonal coupling even when $\ell=0$. This drives transitions between $m_s=\pm1$. Close enough to the axis of the guide, this becomes the dominant interaction so that spin-up and spin-down are completely mixed, as we found in Sec. IV. Likewise, for all higher spins one finds a $\Delta m_s=\pm2$ coupling between the adiabatic states, even when $\ell=0$, and a $\Delta m_s=\pm1$ coupling proportional to $\ell$, but no other off-diagonal terms.

## VI. ADDITIONAL STABILIZING FIELD $B_z$

The spin should be less inclined to flip if we prevent the field from going to zero at the center of the guide by adding a bias field $B_z$ along $z$, but how strong a field is required? A simple physical picture provides the answer. For an atom orbiting at radius $\rho$ with angular momentum $\ell$, the direction of the local magnetic field rotates at frequency $\ell/(m\rho^2)$, whereas the frequency of spin precession around the magnetic field is $G\rho$. The spin becomes unable to follow the local field when the precession frequency is less than the rotation frequency [23]. Therefore we would expect the adiabatic states to be coupled at radii less than a critical value $\rho_c\approx[\ell/(mG)]^{1/3}$, and this is indeed the region where the off-diagonal element in Eq. (5.3) exceeds the characteristic

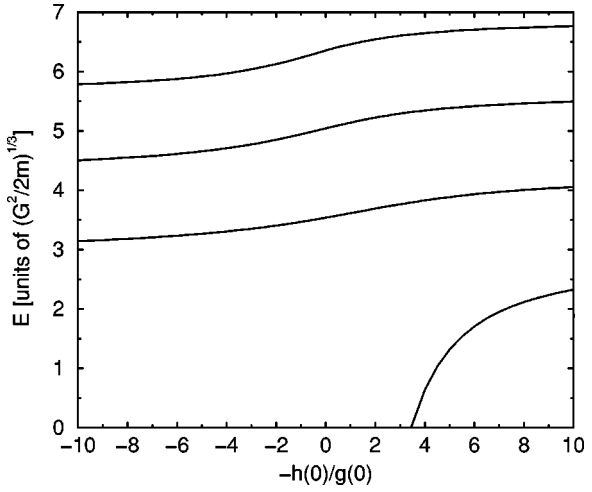


FIG. 6. The first two bands of the $s=1/2, \ell=1$ spectrum versus the boundary condition at the origin. This differs from Fig. 1 because there is now a bias field such that $\mu_B B_z = 1(G^2/2m)^{1/3}$.

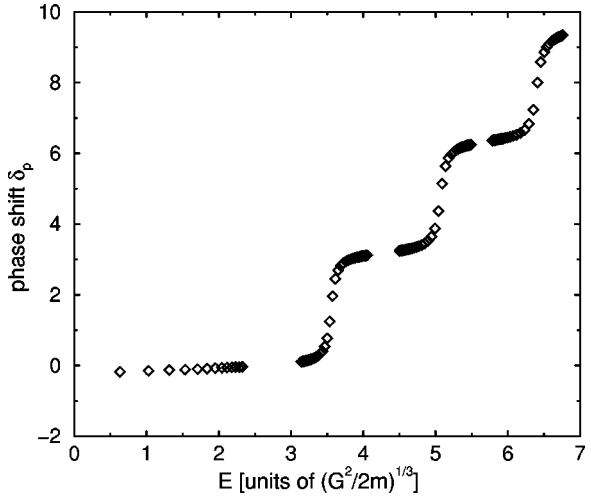


FIG. 7. Phase shift $\delta_p$ for $s=1/2, \ell=1$ in the presence of the bias field. The steps are much steeper than in Fig. 3, which indicates much narrower resonances and consequently a much reduced decay rate as a result of the bias field.

energy $G\rho$ of Eq. (5.1). The addition of a bias field $B_z$ prevents the precession frequency from falling below $\mu_B B_z$ and provides an increasingly constant magnetic field direction as the atom approaches the center of the guide. This is effective out to a radius of order $\mu_B B_z/G$ where the guide field becomes comparable with the bias field. Provided this radius is made larger than the critical value $\rho_c$, we can expect the spin to follow the field adiabatically all the way in to the center, which suppresses the loss of atoms from the guide. This puts a lower limit on the required bias field of $\mu_B B_z \approx \ell^{1/3}$, if $\mu_B B_z$ is measured in natural energy units, $(G^2/2m)^{1/3}$ for spin 1/2. Here we show briefly that this condition is indeed correct for the case of spin 1/2, $\ell=1$.

With the addition of the bias field, the potential $V$ changes from Eq. (3.1) to

$$V=\begin{pmatrix} \mu_B B_z & G\rho e^{i\phi} \\ G\rho e^{-i\phi} & -\mu_B B_z \end{pmatrix}.$$

This additional interaction changes the right-hand side of Eq. (3.7) to give

$$-F_+'' - \frac{F_+'}{\rho} + \frac{\left(\ell+\frac{1}{2}\right)^2 F_+}{\rho^2} + 2mG\rho F_- = 2m(E-\mu_B B_z)F_+,$$

$$-F_-'' - \frac{F_-'}{\rho} + \frac{\left(\ell-\frac{1}{2}\right)^2 F_-}{\rho^2} + 2mG\rho F_+ = 2m(E+\mu_B B_z)F_-. \quad (6.1)$$

For the case of $\ell=1$ we have integrated these equations numerically with $\mu_B B_z = 1$, i.e., the minimum value of $\ell^{1/3}$ estimated above. The new bands of eigenvalues are shown in Fig. 6. These are qualitatively similar to the $\ell=1, B_z=0$ bands in Fig. 1, but their rise is much more gradual. Consequently, the steps near the center of each band encompass a much wider range of spin directions at the origin. The resonances seen in the phase shifts are now very sharp as shown in Fig. 7. We explain in the Appendix how these phase shifts have been calculated. The data of Fig. 7 give a perfect fit to a sum of arctan functions (A10). The energies and widths of the three lowest resonances are (3.55,0.05), (5.07,0.06), and (6.40,0.065). The widths of these resonances correspond to a lifetime of 20 in natural units which shows that the bias field has indeed stabilized the guide as predicted.

Further one can analyze how these widths change with increasing strength of the stabilizing $B_z$ field. We have plotted the widths of the three lowest resonances for $s=1/2, \ell=1$ in Fig 8. The logarithmic scale of the plot shows that the reduction in width with increasing bias field is exponential and that the decay constant is indeed of order $O(1)$ as predicted by the crude estimate made at the beginning of this section.

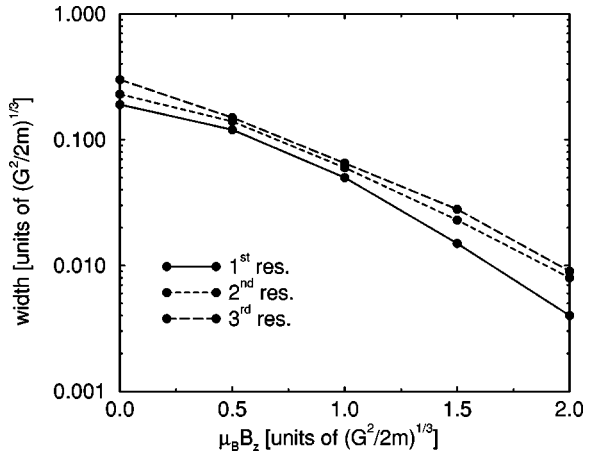


FIG. 8. Widths of the three lowest resonances for $s=1/2, \ell=1$ as a function of the strength of the bias field. The decay constant is approximately 1.7.

## VII. SUMMARY AND CONCLUSIONS

This paper has demonstrated that a magnetic quadrupole atom waveguide can support some stable, bound states of zero orbital angular momentum, even though there is zero magnetic field at the center. For $s=1/2,\ell=0$, these stable states have their spin parallel to the local magnetic field throughout the guide—they are adiabatic spin-up states of the form given in Eq. (3.4)—and the geometric phase associated with the rotation of the spin direction ensures that the atom is kept away from the axis of the guide. The eigenenergies are given by the zeros of the Airy function in accordance with Eq. (3.10).

By contrast, the stable states for $s=1,\ell=0$ are not purely spin-up. At radii greater than unity [in the natural units for $s=1$ of $(4mG/\hbar^2)^{-1/3}$] the spin does follow the local field direction, but close to the center it becomes $m_s=0$ with respect to the $z$ axis. This makes it independent of $\phi$ and therefore insensitive to the azimuthal kinetic energy term $\rho^{-2}\partial^2/\partial\phi^2$ which normally drives the spin flips. In this state the wave function diverges logarithmically on the axis and the eigenenergies are given by Eq. (4.14). We believe that for any integer value of the spin there are similar stable $\ell=0$ states that have spin-up polarization $|\uparrow\rangle$ at large radius and tend to the $\phi$ independent $m_s=0$ on axis. For half-integer spin there do not seem to be stable $\ell=0$ states apart from the special case of spin 1/2.

We have also shown that low-lying states which have nonzero total angular momentum along the guide axis typically decay in a few oscillation periods as a result of spin flips induced by $\rho^{-2}\partial^2/\partial\phi^2$. However, a guide mode of angular momentum $\ell$ can be stabilized by the addition of a uniform field along $z$ of strength $\mu_B B_z \approx \ell^{1/3}$.

Since the bound states that we have discussed in Secs. III and IV are embedded in a continuum of unstable ones, it is possible that practical imperfections of the guide will also induce an appreciable loss rate; this has yet to be determined in the laboratory. The addition of a bias magnetic field along the $z$ axis of the guide can be expected to increase its stability against this kind of loss as well.

Finally, we estimate some practical orders of magnitude to illustrate the relevance of this calculation for possible experiments. Using Eq. (4.14), we can write the first excitation energy for an $\ell=1$ atom of $^{87}$Rb $(s=1,g=-1/2)$ in terms of Planck's constant as $0.32\ I^{2/3}R^{-4/3}h$, where $I$ (A) is the current in the wires and $R$ (m) is their distance from the axis of the guide. It is perfectly practical to have $I=4$ A and $R=500\ \mu$m—indeed such a guide is already being used in our laboratory. Then the first excitation energy for $s=1,\ell=0$ corresponds to a frequency of 20 kHz (or a temperature of 1 $\mu$K), which is large enough to make the quantum-mechanical mode structure an important feature of the dynamics [16]. In such a guide, the bias field required to stabilize states up to $\ell=10$ is less than 10 $\mu$T, but even lower fields could be used if one wanted to filter out all but the lowest angular momentum states. The natural length scale for these parameters, corresponding to the radial extent of the lowest mode, is 70 nm.

## ACKNOWLEDGMENTS

It is a pleasure to thank Gabriel Barton, Malcolm Boshier, and Barry Garraway for discussions, Yvonne Unruh for help with retrieving important literature on differential equations, and James Robbins for help with numerical work. We are indebted to the Royal Society for financial support, and we would like to acknowledge additional funding through research grants from EPSRC and the European Union.

## APPENDIX: WAVE PACKETS AND PHASE SHIFTS

The lifetime of a metastable state is commonly probed by determining the time delay that a wave packet sustains in the interaction region (cf., e.g., Ref. [24]). In the case of the present problem the interaction region is around the center of the guide where spin flips take place, while far away from the center the potential is so strong that the down states $|\downarrow\rangle$ and up states $|\uparrow\rangle$ are not appreciably coupled. To find how long an atom is held in a quasibound state of the guide, one sends a wave packet of $|\downarrow\rangle$ states from large radius towards the axis and measures the time delay of the re-emerging packet. However, standard scattering theory cannot immediately be applied to this problem because the asymptotic solutions of the Schrödinger equation are not plane waves. We therefore outline in this Appendix how wave packets are formed and lifetimes measured in such a system.

For brevity we concentrate on the case of spin 1/2. We rewrite Eq. (3.7) by scaling the radial variable to $\xi=(2mG)^{1/3}\rho$ and by making the substitutions $F_+(\xi)+F_-(\xi)=p(\xi)/\sqrt{\xi}$ for the $|\uparrow\rangle$ component and $F_+(\xi)-F_-(\xi)=q(\xi)/\sqrt{\xi}$ for the $|\downarrow\rangle$ component. This gives

$$-p''+\xi p+\frac{1}{\xi^2}(\ell^2 p+\ell q)=\epsilon p, \tag{A1a}$$

$$-q''-\xi q+\frac{1}{\xi^2}(\ell^2 q+\ell p)=\epsilon q, \tag{A1b}$$

where $\epsilon=(2mG)^{1/3}E/G$ is a shorthand for the energy in natural units. At large $\xi$ the $1/\xi^2$ terms become negligible, which leaves two decoupled Airy equations. Hence the asymptotic solutions of Eqs. (A1a,b) are [21, Sec. 10.4]

$$p(\xi)\overset{\xi\to\infty}{\sim} c_1\,\mathrm{Ai}(\xi-\epsilon)+c_2\,\mathrm{Bi}(\xi-\epsilon),$$

$$q(\xi)\overset{\xi\to\infty}{\sim} d_1\,\mathrm{Ai}(-\xi-\epsilon)+d_2\,\mathrm{Bi}(-\xi-\epsilon).$$

The exponentially growing solution $\mathrm{Bi}(\xi-\epsilon)$ has to be discarded by choosing $c_2=0$. Using asymptotic expansions for the Airy functions of large arguments [21, Sec. 10.4], one finds that

$$p(\xi)\overset{\xi\to\infty}{\sim} c_1\frac{1}{2\sqrt{\pi}}\frac{1}{(\xi-\epsilon)^{1/4}}\ e^{-2/3(\xi-\epsilon)^{3/2}} \tag{A2a}$$

$$q(\xi) \overset{\xi\to\infty}{\sim} d_1 \frac{1}{\sqrt{\pi}} \frac{1}{(\xi+\epsilon)^{1/4}} \sin\left[\frac{2}{3}(\xi+\epsilon)^{3/2}+\frac{\pi}{4}\right] + d_2 \frac{1}{\sqrt{\pi}} \frac{1}{(\xi+\epsilon)^{1/4}} \cos\left[\frac{2}{3}(\xi+\epsilon)^{3/2}+\frac{\pi}{4}\right]. \tag{A2b}$$

As one would expect, the bound $|\uparrow\rangle$ component $p$ is exponentially attenuated at large $\xi$ and the unbound $|\downarrow\rangle$ component $q$ oscillates. An inward-moving $|\downarrow\rangle$ wave $e^{-i\epsilon t}q_{\rm in}(\xi)$ is obtained by choosing $d_1=-i$ and $d_2=1$, i.e.,

$$q_{\rm in}(\xi) \sim \frac{1}{\sqrt{\pi}} \frac{1}{(\xi+\epsilon)^{1/4}} \exp\left\{-i\left[\frac{2}{3}(\xi+\epsilon)^{3/2}+\frac{\pi}{4}\right]\right\}, \tag{A3}$$

while the outward-moving scattered wave $e^{-i\epsilon t}q_{\rm scatt}(\xi)$ that results is described by

$$q_{\rm scatt}(\xi) \sim \frac{1}{\sqrt{\pi}} \frac{1}{(\xi+\epsilon)^{1/4}} \exp\left\{2i\delta+i\left[\frac{2}{3}(\xi+\epsilon)^{3/2}+\frac{\pi}{4}\right]\right\}, \tag{A4}$$

which corresponds to $d_1=ie^{2i\delta}, d_2=e^{2i\delta}$. The sum of incoming and outgoing waves is

$$q(\xi;\epsilon)=q_{\rm in}(\xi)+q_{\rm scatt}(\xi) \sim e^{i\delta}\frac{2}{\sqrt{\pi}} \frac{1}{(\xi+\epsilon)^{1/4}} \cos\left[\frac{2}{3}(\xi+\epsilon)^{3/2}+\frac{\pi}{4}+\delta\right]. \tag{A5}$$

For a fixed energy $\epsilon$ this must be the asymptotic solution of Eqs. (A1a,b), which determines the value of the phase shift $\delta(\epsilon)$.

One can calculate $\delta(\epsilon)$ by integrating Eq. (A1a,b) numerically and determining how the zeros of $q(\xi;\epsilon)$ change with energy. However, only part of this energy-dependent phase shift is due to the coupling to the quasibound states in the $p$ channel. Since the asymptotic solutions at large radius are not plane waves, a nontrivial phase shift arises even when there are no interactions between $p$ and $q$, i.e., when the $\not{p}/\xi^2$ term in Eq. (A1b) is ignored. If one also ignores the angular momentum barrier $\not{q}^2/\xi^2$ and demands that the solution (A5) is valid right down to the center of the guide, $\xi=0$, then the requirement of regularity $q(0;\epsilon)=0$ determines, up to an integer multiple of $\pi$, the phase shift of the noninteracting system as

$$\delta_0=\frac{\pi}{4}-\frac{2}{3}\epsilon^{3/2}. \tag{A6}$$

We note that the inclusion of the angular momentum barrier leads to a constant, i.e., energy-independent, phase shift [25], which we shall ignore in the following since for the calculation of the lifetimes of quasibound states we require only the energy-dependent part of $\delta(\epsilon)$. Writing the total phase shift $\delta$ as a sum $\delta_0+\delta_p$, we find from Eq. (A5) that the phase shift due to the coupling to the quasibound $p$ component is, up to an irrelevant constant, given by

$$\delta_p(\epsilon)=-\frac{2}{3}\{[\xi_0(\epsilon)+\epsilon]^{3/2}-\epsilon^{3/2}\}, \tag{A7}$$

where $\xi_0$ is a zero of the (numerically calculated) solution of the interacting system (A1a,b), i.e., $q(\xi_0)=0$. The data of Fig. 3 have been calculated by tracking the energy dependence of a zero $\xi_0$ and then applying Eq. (A7). It does not matter which zero of the solution one chooses as long as $\xi_0$ is large enough for the asymptotic form (A2a,b) to be applicable.

We now move on to show how $\delta_p$ is related to the lifetime of quasibound states in the $p$ channel, i.e., the $|\uparrow\rangle$ channel. Using Eqs. (A3) and (A4), one can describe a wave packet that comes in, scatters, and goes out again by

$$W(\xi,t)=\int d\epsilon\ a(\epsilon)\ \exp(-i\epsilon t)q(\xi;\epsilon),$$

$$W(\xi,t)\sim\frac{1}{\sqrt{\pi}}\int d\epsilon\ a(\epsilon)\ \exp(-i\epsilon t)\frac{1}{(\xi+\epsilon)^{1/4}} \times\left(\exp\left\{-i\left[\frac{2}{3}(\xi+\epsilon)^{3/2}+\frac{\pi}{4}\right]\right\} +\exp\left\{2i\delta+i\left[\frac{2}{3}(\xi+\epsilon)^{3/2}+\frac{\pi}{4}\right]\right\}\right).$$

The amplitude function $a(\epsilon)$ is chosen such that $W(\xi,t)$ is a wave packet centered around a certain energy $\epsilon_0$. For example, the Gaussian $a(\epsilon)=a_0\exp[-(\epsilon-\epsilon_0)^2/(2\Delta^2)]$ would be suitable. Now we Taylor expand the integrand of $W(\xi,t)$ around $\epsilon_0$, and since we are not interested in the spreading of the wave packet, we do this only up to first order. The result is

$$W(\xi,t)\simeq\frac{1}{\sqrt{\pi}}\frac{1}{(\xi+\epsilon_0)^{1/4}}\left(\exp\left\{-i\epsilon_0 t-i\left[\frac{2}{3}(\xi+\epsilon_0)^{3/2}+\frac{\pi}{4}\right]\right\} \times\Lambda[t+(\xi+\epsilon_0)^{1/2}] +\exp\left\{-i\epsilon_0 t+i\left[\frac{2}{3}(\xi+\epsilon_0)^{3/2}+\frac{\pi}{4}\right]+2i\delta(\epsilon_0)\right\} \times\Lambda\left[t-(\xi+\epsilon_0)^{1/2}-2\frac{\partial\delta}{\partial\epsilon}\right]\right) \tag{A8}$$

with

$$\Lambda(\tau)\equiv\int d\epsilon\ a(\epsilon)\ e^{-i(\epsilon-\epsilon_0)\tau}.$$

The function $\Lambda(\tau)$ peaks near $\tau\approx 0$. Consequently, of the two terms in Eq. (A8), only the first one—the incoming

wave packet—peaks for large negative times, whereas the outgoing second term has the peak at large positive times. If the interaction with the $p$ channel is switched off, the packet goes right through the origin and the phase shift of the outgoing packet is $\delta_0$ of Eq. (A6), which ensures continuity at $\xi=0$. By comparison, any additional phase shift due to the interaction with the $p$ channel causes a time delay $Q$ of the outgoing packet:

$$Q=2\frac{\partial}{\partial\epsilon}(\delta-\delta_0)=2\frac{\partial\delta_p}{\partial\epsilon}. \tag{A9}$$

When there is a resonance at energy $\epsilon_p$ in the $p$ channel, the function $Q(\epsilon_p)$ has a peak because part of the wave packet is held in the quasibound state and therefore delayed by the lifetime of that state. Equivalently, $Q^{-1}$ has a dip which we can Taylor expand around $\epsilon_p$ as

$$Q^{-1}(\epsilon)\simeq\alpha+\beta(\epsilon-\epsilon_p)^2$$

with positive $\alpha$ and $\beta$. Using this in Eq. (A9) one obtains

$$\delta_p(\epsilon)=\frac{1}{2\sqrt{\alpha\beta}}\left[\arctan\left(\sqrt{\frac{\beta}{\alpha}}(\epsilon-\epsilon_p)\right)+\frac{\pi}{2}\right],$$

a step of height $\pi/(2\sqrt{\alpha\beta})$ and width $\Gamma=\sqrt{\alpha/\beta}$. Since far away from the resonance the wave packets must be equivalent solutions of the noninteracting system, one can infer the height of the step to be $\pi$, because this is the smallest value whose addition to $\delta$ leaves $q_{\mathrm{scatt}}(\xi)$ of Eq. (A4) invariant. Consequently, $2\sqrt{\alpha\beta}=1$ and the width $\Gamma$ is related to the time delay $Q(\epsilon_p)=1/\alpha$ through

$$\Gamma^{-1}=\frac{1}{2}Q(\epsilon_p).$$

Hence a fit of the numerically calculated phase shift of Fig. 3 to a sum of arctan functions,

$$\delta_p=\sum_i\left[\arctan\left(\frac{\epsilon-\epsilon_i}{\Gamma_i}\right)+\frac{\pi}{2}\right], \tag{A10}$$

lets one determine the energies $\epsilon_i$ and the lifetimes $\Gamma_i^{-1}$ of the resonances.

The above considerations apply almost unaltered to the system of Sec. VI with the additional stabilizing field $B_z$. With the same substitutions as before, system (6.1) is transformed into

$$-p''+\xi p+\frac{1}{\xi^2}(\not{\partial}^2 p+\not{\partial} q)=\epsilon p-\kappa q,$$

$$-q''-\xi q+\frac{1}{\xi^2}(\not{\partial}^2 q+\not{\partial} p)=\epsilon q-\kappa p,$$

where $\kappa=(2mG)^{1/3}\mu_{\mathrm{B}}B_z/G$. Unfortunately, the asymptotics of this system cannot be deduced from known special functions but must be derived from scratch. To this end we ignore the $1/\xi^2$ terms, and then insert the first into the second equation, which gives a fourth-order differential equation for $q(\xi)$:

$$-q^{(4)}-2\epsilon q''+(\xi^2-\epsilon^2+\kappa^2)q=0.$$

This equation has an irregular singular point at $\xi\to\infty$, so that its asymptotics must be of the form [26, Secs. 3.4–5]

$$q(\xi)\overset{\xi\to\infty}{\sim}e^{S(\xi)}. \tag{A11}$$

Using this ansatz and observing that in deriving the leading asymptotic behavior one can neglect $S''$ compared to $(S')^2$ and likewise $S^{(n)}\ll(S')^n$ for all $n\geqslant 2$ because $S(\xi)$ must increase faster than logarithmic [26, Sec. 3.4, Example 5], one gets the four solutions

$$S'(\xi)=\begin{cases}\pm\sqrt{\sqrt{\xi^2+\kappa^2}-\epsilon}\\ \pm i\sqrt{\sqrt{\xi^2+\kappa^2}+\epsilon}.\end{cases}$$

Since the spin-down component $q(\xi)$ is a traveling wave, we must choose the lower line of this solution for $S'$. Integrating and inserting it into Eq. (A11) we obtain the equivalent of Eq. (A2b) for the case with the stabilizing field $B_z$. Proceeding along the same lines as before, we derive the phase shift due to the coupling to the quasibound states in the $p$ channel

$$\delta_p=-\int_0^{\xi_0(\epsilon)}d\xi\sqrt{\sqrt{\xi^2+\kappa^2}+\epsilon}, \tag{A12}$$

which is the formula we have used in generating the data in Fig. 7. We note that in the limit $B_z\to 0$ Eq. (A12) reverts to Eq. (A7), as it must.


[1] C. S. Adams and E. Riis, Prog. Quantum Electron. **21**, 1 (1997).

[2] J. P. Dowling and J. Gea-Banacloche, Adv. At., Mol., Opt. Phys. **37**, 1 (1996).

[3] V. I. Balykin, Adv. At., Mol., Opt. Phys. **41**, 181 (1999).

[4] R. J. Cook and R. K. Hill, Opt. Commun. **43**, 258 (1982).

[5] M. J. Renn *et al.*, Phys. Rev. A **53**, R648 (1996); M. J. Renn *et al.*, *ibid.* **55**, 3684 (1997); H. Ito *et al.*, Appl. Phys. Lett. **70**, 2496 (1997).

[6] M. J. Renn *et al.*, Phys. Rev. Lett. **75**, 3253 (1995).

[7] E. A. Hinds and I. G. Hughes, J. Phys. D **32**, R119 (1999).

[8] T. Bergeman, G. Erez, and H. Metcalf, Phys. Rev. A **35**, 1535 (1987).

[9] N. Masuhara *et al.*, Phys. Rev. Lett. **61**, 935 (1988).

[10] W. Ketterle, D. S. Durfee, and D. M. Stamper-Kurn, e-print cond-mat/9904034; E. A. Cornell, J. R. Ensher, and C. E.

Wieman, e-print cond-mat/9903109.
[11] H. Friedburg, Z. Phys. **130**, 493 (1951); H. Friedburg and W. Paul, Naturwissenschafen **38**, 159 (1951).
[12] L. V. Hau, J. A. Golovchenko, and M. M. Burns, Phys. Rev. Lett. **75**, 1426 (1995); K. Berg-Sorensen, M. M. Burns, J. A. Golovchenko, and L. V. Hau, Phys. Rev. A **53**, 1653 (1996).
[13] J. Schmiedmayer, Phys. Rev. A **52**, R13 (1995).
[14] J. A. Richmond *et al.*, Acta Phys. Slov. **48**, 481 (1998).
[15] J. Denschlag, D. Cassettari, and J. Schmiedmayer, Phys. Rev. Lett. **82**, 2014 (1999).
[16] M. Olshanii, Phys. Rev. Lett. **81**, 938 (1998).
[17] H. Monien, M. Linn, and N. Elstner, Phys. Rev. A **58**, R3395 (1998).
[18] Throughout this paper we take $\hbar=1$ unless explicitly indicated.
[19] W. Petrich *et al.*, Phys. Rev. Lett. **74**, 3352 (1995).
[20] D. M. Brink and G. R. Satchler, *Angular Momentum* (Clarendon, Oxford, 1961).
[21] *Handbook of Mathematical Functions*, edited by M. Abramowitz and I. A. Stegun (U.S. G.P.O., Washington, DC, 1964).
[22] Here we have restored $\hbar$ to show that $(2mG/\hbar^2)^{-1/3}$ is a characteristic length for this problem.
[23] E. Majorana, Nuovo Cimento **8**, 43 (1932).
[24] M. L. Goldberger and K. M. Watson, *Collision Theory* (Wiley, New York, 1964).
[25] The phase shift due to the angular momentum barrier can be seen to be equal to $-\sqrt{1+4\ell^2}\pi/4$ by solving Eq. (A1b) for $p\equiv 0$ and $\xi \ll \epsilon$. In this limit one finds $q(\xi)\sim\sqrt{\xi}J_\nu(\sqrt{\epsilon}\xi)$ with $\nu=\sqrt{1+4\ell^2}/2$, and thus for $\sqrt{\epsilon}\xi \gg \nu$ one obtains $q(\xi)\sim\cos(\sqrt{\epsilon}\xi-\sqrt{1+4\ell^2}\pi/4-\pi/4)$.
[26] C. M. Bender and S. M. Orszag, *Advanced Mathematical Methods for Scientists and Engineers* (McGraw-Hill, Singapore, 1978).